Computationally effective range migration compensation in PCL systems for maritime surveillance

T. Martelli, F. Filippini, F. Pignol, F. Colone
DIET Dept. Sapienza University of Rome,
Via Eudossiana 18, 00184 Rome, Italy
{tatiana.martelli, francesca.filippini,fabiola.colone}@uniroma1.it

Roberta Cardinali
Leonardo Company
Via Tiburtina Km 12.400, 00131 Rome (Italy)
roberta.cardinali@leonardocompany.com

***Abstract* — In this paper, we consider the possibility of extending the coherent processing interval (CPI) as a way to improve target detection capability in passive radars for maritime surveillance applications. Despite the low velocity of the considered targets, range walk effects could limit the performance of the system when long CPIs are considered. To overcome these limitations while keeping the computational load controlled, we resort to a sub-optimal implementation of the Keystone Transform (KT), based on Lagrange polynomial interpolation, recently presented by the authors and successfully applied against aerial targets. Following those promising results, we extend the proposed approach to a coastal surveillance scenario. In the considered case, since longer CPI values are used, the proposed strategy appears to be even more attractive with respect to a conventional KT implementation based on the Chirp-Z Transform interpolation. In fact, comparable detection performance are obtained with a remarkable computational load saving. In detail, the effectiveness of the proposed approach is demonstrated against experimental data provided by Leonardo S.p.A., using a DVB-T based passive radar.**

Keywords—passive radars, long coherent processing interval, range migration compensation, Keystone Trasform.

I. INTRODUCTION

Nowadays Passive Radars (PR), often also referred to as Passive Coherent Location (PCL) systems, have reached a point of maturity and their effectiveness has been demonstrated for civilian, security and defense applications. Specifically, the exploitation of PR systems in coastal/maritime surveillance applications has recently received significant interest from the passive radar community [1]-[6].

For instance, terrestrial sources such as DVB-T and GSM have been shown to be a suitable alternative to the expensive and intrusive active systems for coastal surveillance purposes. As reported in [1]-[2], such sensors can be employed for monitoring typical maritime traffic as well as for detecting small boats close to the coast. Furthermore, due to the low carrier frequencies of the DVB-T waveforms, the over the horizon (OTH) capability has been investigated in [3]-[4], showing that a DVB-T based PR can be successfully employed even in very long range maritime surveillance applications. Recently, satellite illuminators of opportunity have been also considered as sources of opportunity in order to allow radar coverage of open sea areas [5]-[6].

In this paper, we consider a DVB-T based PR for maritime surveillance. Thanks to the orthogonal frequency division multiplexing (OFDM) modulation based on persistent sub-carriers that span a total bandwidth of up to 8 MHz, a quite stable range resolution of approx. 20 m (equivalent monostatic value) is obtained. This means that in the considered application, the low velocity of potential targets allows to increase the Coherent Integration Interval (CPI) duration up to 1-2 seconds without experiencing significant range migration effects. However, aiming at enhancing the detection of targets with low Signal to Noise Ratio (SNR), or in order to broaden the coverage area, one could use longer CPIs by properly correcting the range migration effects.

As reported in [7]-[11], by taking inspiration from original algorithms defined for active radar systems, different techniques have been proposed to counteract this problem in PR systems. Among them, the authors recently resorted to the well-known Keystone Transform (KT) to compensate for the range walk and to take advantage of a higher coherent integration gain against targets with non-negligible radial velocity [12]. Specifically, an efficient implementation of the KT was proposed based on Lagrange P-order polynomial interpolation (P-LPI), in order to reduce the computational load of the method that mostly depends on the required slow-time interpolation stage. The analysis conducted against real air traffic data showed that the conceived sub-optimal approach allows to achieve comparable target detection performance with respect to alternative solutions based on cardinal sine functions or Chirp-Z Transforms (CZT) while reducing the KT complexity.

In this paper, we extend the study in [12] by evaluating the benefits of the proposed strategy against maritime targets. First, we optimize the relevant parameters to make them effective in the considered scenario. Then, we evaluate the computational complexity required by different algorithms in order to investigate the efficiency of the proposed sub-optimal range migration compensation technique. Finally, we demonstrate the effectiveness of the proposed scheme against experimental data provided by Leonardo S.p.A. The experimental results show that a simple 1-LPI based KT allows comparable detection performance with respect to the optimal CZT based KT with a substantial reduction of the computational burden.

The paper is organized as follows. In Section II we briefly summarize the application of the KT in the passive radar together with the different interpolation strategies to compensate the range migration. An analysis on the selection of the relevant parameters to be effective in the considered scenario is reported in Section III together with the analysis of the computational load. Then, the experimental results are illustrated in Section IV. Finally, our conclusions are drawn in Section V.

II. RANGE MIGRATION COMPENSATION VIA KT

A. Basic DVB-T based PR processing scheme and limitations of the integration time

A basic DVB-T PR processing scheme features a first disturbance cancellation stage, after which the target detection is sought by evaluating the bistatic range-Doppler Cross-Ambiguity Function (CAF) between the surveillance signal $s(t)$ and the reference signal $r(t)$. Assuming that the signals are sampled at frequency f_s, the resulting range/Doppler maps can be expressed in discrete time notation as:

$$\chi[l,m] = \sum_{n=0}^{N_{CIT}-1} s[n]r^*[n-l]\exp\left(-j2\pi\,\frac{mn}{N_{CIT}}\right) \quad (1)$$

where N_{CIT} is the number of integrated samples and defines the CPI $= N_{CIT}/f_s$, l represents the range bin and m the Doppler bin. Depending on the considered surveillance application, the CPI is carefully selected to limit the expected range and Doppler migration on the targets of interest. For instance, in a maritime scenario, the low velocity of potential targets allows to increase the CPI up to a 1-2 seconds without experiencing significant migrations [3]-[4].

Aiming at increasing the target SNR or at extending the radar coverage, one could consider longer CPIs, which allow to improve the Doppler resolution as well as the capability to discriminate between slowly moving vessels and docked boats. However, the range walk effects must be taken into account. In fact, due to the fine range resolution offered by the DVB-T signals, even targets characterized by low bistatic velocity (15-20 m/s) might migrate across the range cells. In [12] the authors proposed an effective implementation of the KT, based on the Lagrange polynomial interpolation approach, achieving comparable detection performance with respect to the optimal CZT-based KT, whilst significantly reducing the computational load. The proposed approach is briefly described below.

B. P-LPI-based KT for PR case

The KT technique is widely used in active radar to compensate for the range migration. It can be applied to PR systems employing continuous wave (CW) transmissions by resorting to a batches approach (see Fig. 1). In fact, as reported in [13], (1) can be rewritten as:

$$\chi[l,m] = \sum_{n=0}^{N_B-1}\sum_{q=0}^{L_B-1} s[nL_B+q]r^*[nL_B+q-l] \times \exp\left[-j2\pi\,\frac{m(nL_B+q)}{N_{CIT}}\right] \quad (2)$$

where the index n defines the slow-time domain and the index q indicates the fast-time. Specifically, the received signals are subdivided into N_B batches of L_B samples each (with $L_B N_B = N_{CIT}$).

Neglecting the Doppler linear compensation within each batch, we obtain:

$$\chi[l,m] \cong \sum_{n=0}^{N_B-1}\exp\left[-j2\pi\,\frac{mn}{N_B}\right] \times \sum_{q=0}^{L_B-1} s[nL_B+q]r^*[nL_B+q-l] \quad (3)$$

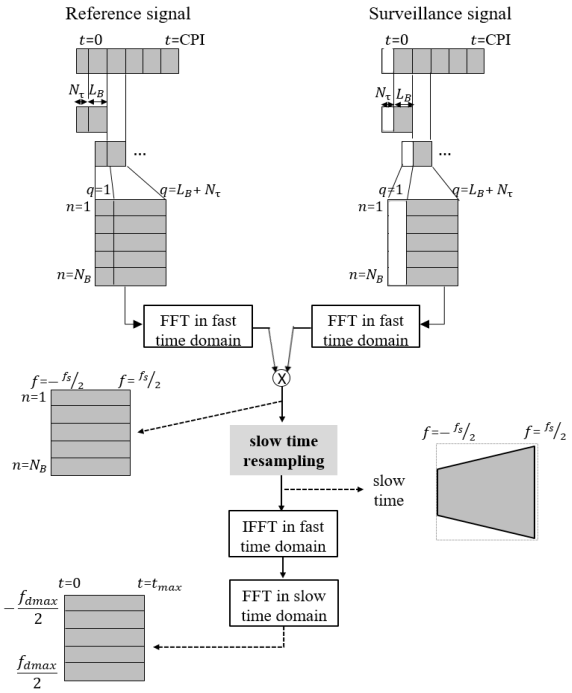

Fig. 1. Bistatic range/Doppler map evaluation in passive radar system with a batches architecture based Keystone Transform for range migration compensation.

The above approximation yields a SNR loss that we can control by properly selecting the batches length L_B of duration equal to $T_B = \frac{L_B}{f_s}$ [13].

The inner summation in (3) represents the cross-correlation function between the surveillance and the reference signals, extracted at the *n*-th batch. It can be equivalently evaluated as the IFFT of the product of the individual FFTs (see Fig. 1).

When range walk effects appear, the target echoes migrate along the delay (fast-time) dimension across consecutive batches (slow-time). Aiming at compensating this effect, the KT operates in the fast-time Fourier transformed (namely the fast-frequency) domain. Specifically, as reported in [12], assuming that the surveillance signal only contains the returns from a point-like target with unitary amplitude and constant bistatic velocity, i.e. with a linear bistatic range law $R_B(t) = \alpha_0 + \alpha_1 t$, the data matrix in the fast-time Fourier transformed domain can be written as:

$$D_{ft-FT}[n,p] = P_{ref}^{(n)}[p]\exp\left[j2\pi\,\frac{p}{T_B}\frac{\alpha_0}{c}\right]\exp\left[j2\pi np\,\frac{\alpha_1}{c}\right] \times \exp\left[j2\pi n f_C\,\frac{\alpha_1}{c}T_B\right] \quad (4)$$

where $P_{ref}^{(n)}[p]$ is the Fourier transformed auto-correlation of the reference signal, namely the power spectral density of the signal estimated at the *n*-th batch. The second exponential factor in (4) is the one encoding the range migration effect as it jointly depends on the batch number *n* and on the fast-frequency index p (i.e. on the frequency component displacement, $\Delta f_p = \frac{p}{T_B}$, with respect to the carrier frequency f_C). As it is well known, the KT compensate for this term by rescaling the slow-time (i.e.

interpolating the slow-time samples sequences) according to the following rule:

$$\bar{n} = \frac{f_C + \Delta f_p}{f_C} n \tag{5}$$

As is apparent from Fig. 1, after a fast-time inverse Fourier Transform and a slow-time Fourier Transform, we obtain the bistatic range/Doppler map with range migration correction for any given target bistatic velocity. With respect to the Batches Algorithm (BA) without range migration compensation, only an additional processing block for slow-time resampling is required by the KT. Obviously, this represents a computationally intensive processing stage since it has to be performed at each fast-frequency bin.

To reduce the computational load of the KT slow-time resampling stage, in [11] the CZT was adopted allowing optimal performance with a limited computational complexity. Aiming at further reducing the computational burden, in [12] we presented an alternative interpolation method that uses Lagrange *P*-order polynomials. Therefore, we can write the *P*-LPI based resampling of (4) as:

$$D_{ft-FT}[\bar{n}, p] = \sum_{n=\lfloor \bar{n}-(P+1)/2 \rfloor}^{\lfloor \bar{n}+(P+1)/2 \rfloor} D_{ft-FT}[n, p] \left(\prod_{m=0, m \neq n}^{P} \frac{\bar{n} - n}{n - m} \right) \tag{6}$$

where P is the order of the polynomial adopted and $D_{ft-FT}[n, p]$ is the slow-time/fast-frequency data matrix in (4). In detail, only P+1 consecutive samples in the slow-time domain are exploited to evaluate each interpolated sample according to a P-order polynomial. This means that as we reduce the polynomial order, we reduce the computational load. Clearly, this is paid in terms of SNR loss on the detected target echo. However, with a trade-off between the batch dimension and the polynomial order, negligible losses can be achieved.

III. Parameters Optimization for Maritime Application

The range migration compensation techniques described in Section II are based on a batches architecture. Therefore, we obtain a SNR loss on the considered target with respect to the use of the conventional CAF evaluation. We recall that this loss can be written as follows:

$$Loss = -20 \log_{10} \left| \frac{sin\left(\frac{\pi m L_B}{N_{CIT}}\right)}{L_B \; sin\left(\frac{\pi m}{N_{CIT}}\right)} \right| \tag{7}$$

As is evident, the loss in (7) can be controlled by properly selecting the number of samples L_B in each of the N_B batches. In this work, we forced the SNR loss to be approx. 0.2 dB for a target moving at 10m/s along the X axis. By imposing this constraint, a $L_B = 28312$ has been obtained, which corresponds to a time duration of 0.3 ms. Obviously, a comparable SNR loss is obtained when a CZT based KT is employed. Correspondingly, a maximum SNR loss of 1 dB is yield even using the 1-LPI based KT.

With this choice of L_B, the reduction offered by the P-LPI based KT approach in terms of computational burden is substantial for polynomial order values less than 3. The computational load, that depends on the parameters N_B, L_B as well as the number N_τ of delay bins included in the range/Doppler map, is here reported in terms of number of complex multiplications, for the different approaches [12]:

- BA: $N_B\left[3(L_B + N_\tau) log_2(L_B + N_\tau) + L_B + N_\tau\left(1 + log_2(N_B)\right)\right]$
- CZT-based KT: $N_B \left[3(L_B + N_\tau) log_2(L_B + N_\tau) + L_B + N_\tau \right] + (L_B + N_\tau)\left[4N_B + 2\mathrm{N_B}\left(1 + 3log_2(2N_B)\right)\right]$
- *P*-LPI based KT: $N_B\left[3(L_B + N_\tau) log_2(L_B + N_\tau) + L_B + N_\tau\left(1 + log_2(N_B)\right)\right] + N_B(L_B + N_\tau)\left((P+1)2P\right)$

By setting $N_\tau = 2439$ (we assumed the maximum bistatic range of interest to be $80km$), and the properly selected L_B, we report in Fig. 2 the computational complexity as a function of the CPI. Specifically, the computational burdens required by the following approaches are compared: the P-LPI based KT, with P = [1,3,5,7]; the CZT based KT and the BA.

As is apparent from Fig. 2, by accepting the small loss measured above, the 1-LPI approach (in blue) only requires a slight increase of computational complexity with respect to the BA (in dashed-dot black). In other words, with this approach only a few additional operations are required in order to provide the additional range migration compensation capability. On the other hand, the computational load required by the CZT method (in dashed red) is distinctly higher. Notice that, the higher the CPI, the biggest is the reduction in terms of computational complexity offered by the proposed technique with respect to the CZT-based KT. As an example, when a CPI of 5 s is considered, the CZT technique requires to triple the complex multiplications. It is worth mentioning that even applying an efficient implementation [13], the evaluation of a Conventional CAF requires a computational cost of $4.85 \cdot 10^{11}$ for CPI= 5 s. This limit, along with its incapability of compensating the range walk effects, makes this approach unsuitable for practical applications. However, we will consider it in the following as a benchmark for the performance when no migration is included.

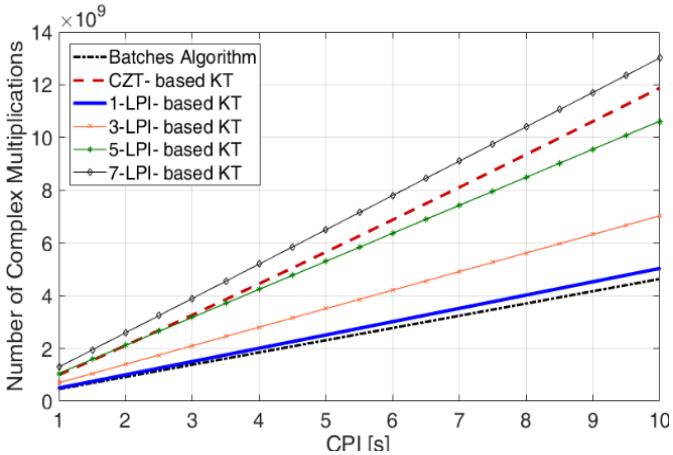

Fig. 2. Comparison of the computational load required by different algorithms as a function of the CPI, when using $L_B = 28312$ s.

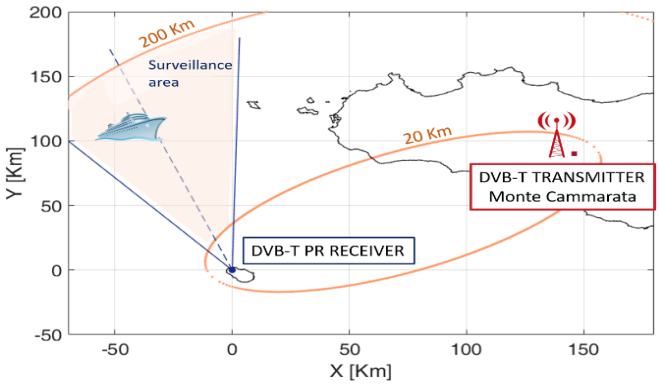

Fig. 2. Sketch of the acquisition geometry.

IV. Results against Experimental Data

We processed a real data set collected by a DVB-T based PR, developed by Leonardo S.p.A. in order to show the benefits of the proposed technique in a maritime surveillance scenario.

A. Acquisition campaign

We conducted an acquisition campaign in Pantelleria, a small island in the South of Italy (see Fig. 3). The exploited illuminator of opportunity is a DVB-T transmitter located in Monte Cammarata (approx. 170 km far from the receiver), emitting signals at a carrier frequency of 690 MHz, while the DVB-T-based PR receiver was installed very close to the coast.

Two Yagi-Uda antennas were employed, with a distance of $0.63\ m$ in the horizontal plane, pointed at $343°$ clockwise from north and main beam width of approx. $36°$. In this way, the considered sensor is able to detect the typical maritime traffic that is present in that area.

The considered data set is composed by a total amount of 101 consecutive data files (scans). Each scan has a temporal duration equal to 4.7s and consecutive scans are spaced by 7s. In addition, the Automatic Identification System (AIS) was adopted during the test in order to record the maritime traffic. Among the available targets of opportunity, we only consider the ones characterized by sufficiently high velocities, namely targets that could be subjected to range migration effects when large CPI are used. According to this criterion, we identified two Cargo vessels which characteristics are reported in Table I. The availability of truth-data for these two non-cooperative targets allowed us to carry out a quantitative analysis to evaluate the target detection improvement resulting from the correction of the range migration. Specifically, we define a given detection as "correct" when it appears at both expected range-velocity location and expected time instant.

B. Analysis of target detetion capability

All the available data files have been processed according to the DVB-T PR processing scheme developed by the authors and presented in [3]-[4].

Specifically, the sliding version of the extensive cancellation algorithm (ECA-S) [14] is adopted for the removal of the undesired contributions at the surveillance channel (i.e. direct signal and multipath echoes). This operates over a range of 33 km (1000 taps @ fs=64/7 MHz) with a batch duration

TABLE I. SPECIFICATIONS ON THE TWO CONSIDERED TARGETS OF OPPORTUNITY.

		Target #1: Morning Lena	Target #2: Kherrata
Specifications	Type	Cargo	Cargo
	Length [m]	232.38	138.41
	Width [m]	32.26	21
	Bistatic Range [km]	52 - 62	36- 43
	Bistatic Velocity [m/s]	15	10
	Photo		

equal to 0.1 s whereas the filter update rate is 10 ms. After the cancellation stage, the output signals from the ECA filter are exploited in order to evaluate the bistatic range/velocity map. To this purpose a properly filtered reference signal is employed in order to remove the high side-lobes and spurious peaks appearing in the DVB-T signal ambiguity function. To this end, we use the approach proposed in [15].

The different algorithms to evaluate the range-velocity map will be compared, using different CPI values. Specifically, due to the maximum data file temporal duration of 4.7s, the CPI has been extended up to 4.5 s. First, the conventional CAF is evaluated by resorting to the Correlation FFT algorithm [13]. Then, the two strategies described in Section II to compensate the range walk are applied with the properly selected batch length L_B.

Fig. 4 reports a zoom of the range-velocity maps of the target #1 obtained at a single scan when different algorithms and CPI are adopted. All the reported maps have been normalized to the thermal noise power level so that each value represents the estimated SNR. We observe that when we use a CPI of 1 s, the peak values measured on the maps are comparable for the different processing schemes (see Fig. 4(a)-(c)). Notice that, the small loss of the CZT-based KT and 1-LPI based KT with respect to the conventional CAF is due to the use of the batches architecture which introduce a limited target SNR loss. In contrast, when we extend the CPI up to 4.5 s (Fig. 4(d)-(f)), the benefits provided by the range migration compensation techniques are visible on the target peak value. In fact, a SNR improvement of 1.15 dB and 0.75 dB are obtained when operating with CZT-based KT and 1-LPI based KT approaches (see Fig. 4(e)-(f)) with respect to the case of no range migration compensation (see Fig. 4(d)). This shows that the range walk effects cannot be neglected in such scenario when increasing the integration time.

Once the bistatic range-velocity maps have been evaluated, a conventional Cell Average – Constant False Alarm Rate (CA-CFAR) threshold is separately applied to each map with a probability of false alarm equal to $Pfa = 10^{-4}$. Then, a two-

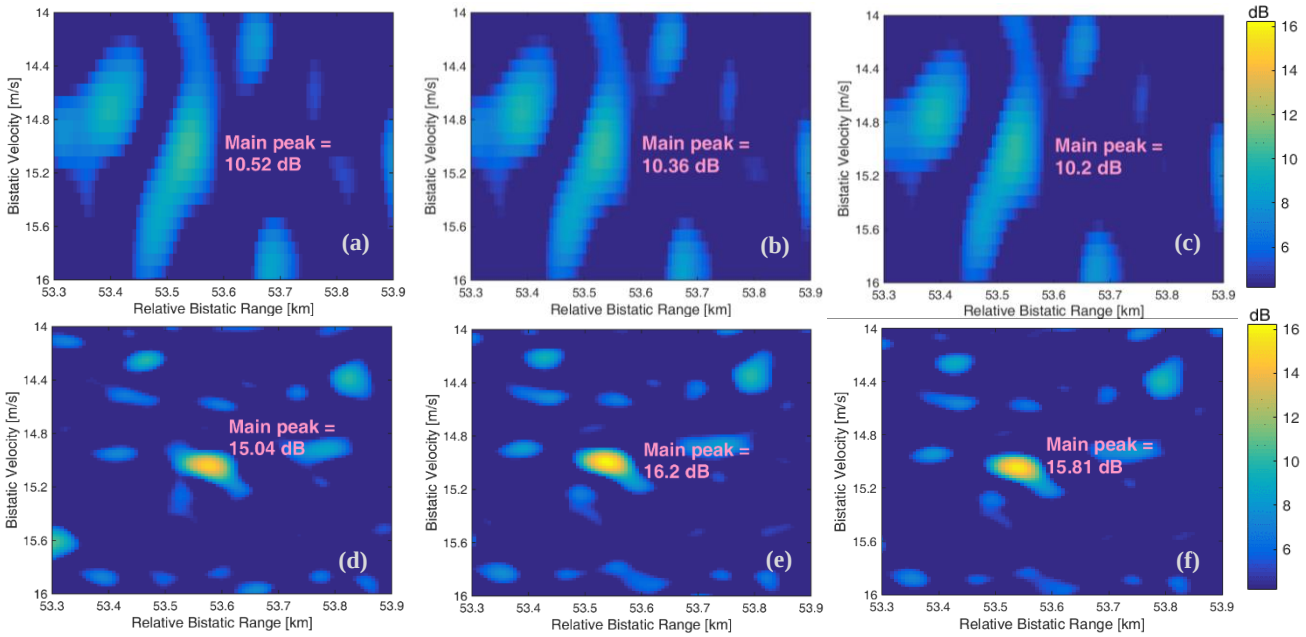

Fig. 3. Zoom of the range-velocity maps of the target #1 obtained at a single scan with different algorithms: (a) Conventional CAF with CPI=1 s; (b) CZT-based-KT with CPI=1 s; (c) 1-LPI-based-KT with CPI=1 s; (d) Conventional CAF with CPI=4.5 s; (e) CZT-based-KT with CPI=4.5 s; (f) 1-LPI-based-KT with CPI=4.5 s.

out-of-two criterion is adopted to integrate the detection results obtained at the two surveillance channels allowing a nominal $Pfa = 10^{-8}$ on the final range-velocity plane.

In Fig. 5 we show the raw detections for target #1 (out the considered 101 consecutive scans), over the range - velocity plane, for a CPI of 1s or 4.5s and using the different strategies described. The red dots represent the PR plots, while the grey line represents the AIS trajectory of the considered target. The same results are also included in Table II, where the detection results of both targets are reported and the three considered processing schemes are compared for the considered CPI values, namely 1s, 2s and 4.5s. Notice that, in each case, the first portion of each data file is exploited thus the number of the observations is kept constant for the different CPI. By observing Table II, the following considerations are in order:
(i) as the CPI increases, a remarkably higher amount of correct target detections is obtained on both targets for all the considered processing schemes. This shows that the coherent integration is an effective strategy to recover the targets showing a low SNR, at least for the considered CPI values and the considered targets.
(ii) When CPI = 1 s, a comparable amount of detections is offered by the three processing schemes for both targets. This result is well in line with the expectations, since no range migration effect is experienced by the considered targets when such value of integration time is considered, i.e. there is no need of applying any range migration compensation. Notice that, with reference to the first target, the two range migration compensation schemes lose one correct detection with respect to the Conventional CAF. This small loss may be due to the fact that both the CZT and the 1-LPI based KT methods include the use of the BA technique to evaluate the range-velocity map and we recall that the BA introduces a small loss on the target SNR. Incidentally, we recall the the Conventional CAF approach requires a substantially higher computational load with respect to the BA strategy.
(iii) When CPI = 2 s, a slight improvement is offered when compensating the range walk on target #1, characterized by the highest velocity (see Table I). On the other hand, it is still not necessary to compensate the range migration for target #2.
(iv) When CPI = 4.5 s, the range migration walk cannot be neglected for either target, i.e. a range migration compensation has to be performed. Specifically, for target #1, we obtain 5 and 7 additional detections with respect to the Conventional CAF when the range migration is compensated by means of the 1-LPI and the CZT based KT, respectively (see Table II and Fig. 5(b-c). As expected, the 1-LPI based KT approach offers a slightly reduced amount of correct detections with respect to the best performing CZT based KT. However, we recall that one could either reduce the loss of the proposed approach by increasing the polynomial order, or exploit the terrific reduction in terms of computational burden to evaluate the maps more frequently (assuming that the maps evaluation is the most expensive stage). For instance, in this case, we could process

TABLE II. DETECTION RESULTS FOR BOTH TARGETS USING DIFFERENT CPI AND DIFFERENT ALGORITHMS FOR RANGE-VELOCITY MAP EVALUATION.

	Target #1			**Target #2**		
	Conventional CAF	***CZT based KT***	***1-LPI based KT***	***Conventional CAF***	***CZT based KT***	***1-LPI based KT***
CPI = 1 s	23	22	22	39	39	39
CPI = 2 s	39	42	41	47	47	47
CPI = 4.5 s	56	63	61	59	64	62

twice as many scans (see Section III). It is worth noticing that, in the considered scenario, the benefits offered by the joint exploitation of long CPI and range migration compensation techniques are not as evident as the aerial case in [12]. This marginal improvement is due to the availability of the considered dataset, namely no high targets velocity and limited data files duration. Despite this, the reported results shown that the range walk effects cannot be neglected. In fact, the proposed range migration compensation approaches allows a target SNR improvement as well as a higher number of detections.

V. Conclusions

In this work, we address the problem of compensating the range walk effect, experienced by the targets when long coherent processing intervals are considered. Specifically, we resort to a computationally effective implementation of the Keystone Transform, based on Lagrange polynomial interpolation. Following the promising results obtained by the authors against aerial targets in [12], we extend the range of application of the proposed approach to a maritime surveillance scenario. The effectiveness of the conceived technique has been shown against experimental data provided by Leonardo S.p.A. and collected by means of a DVB-T based PR. We show that, as the CPI value increases, the benefits obtained with the proposed 1-LPI based KT approach become more apparent. In fact, the longer the CPI, the bigger is the advantage in terms of computational complexity with respect to the conventional CZT based KT interpolation. However, the analysis reported in this work shows preliminary results, obtained with the maximum CPI value allowed by the considered data set. Future works will consider an extensive analysis of the performance, against a higher number of targets and longer CPI, in order to assess the benefits of the proposed approach.

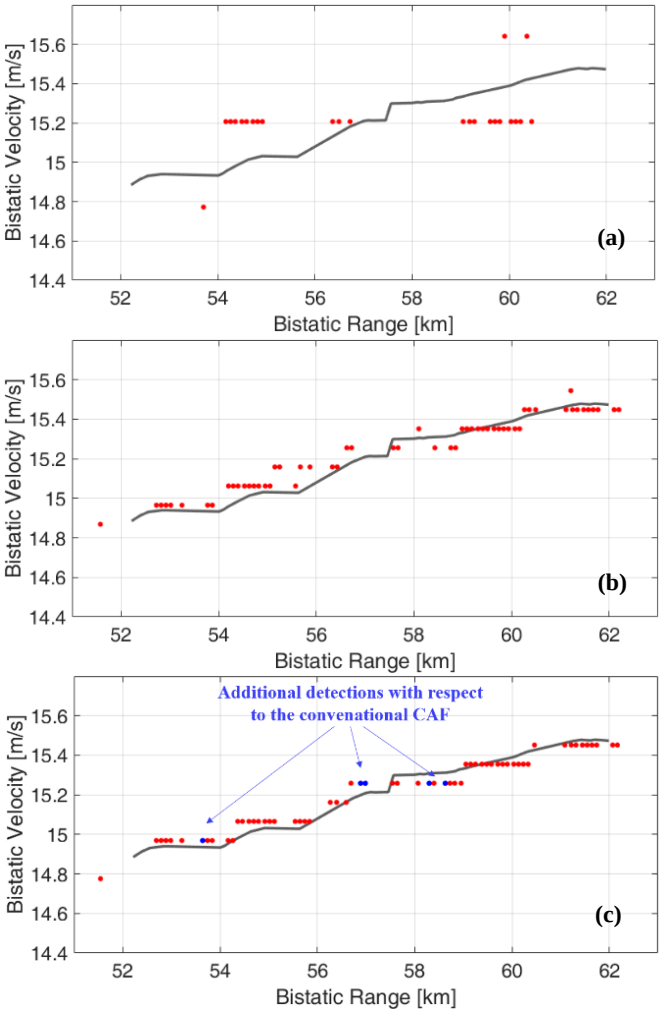

Fig. 4. Detection results on Target #1, using: (a) Conventional CAF with CPI = 1 s; (b) Conventional CAF with CPI = 4.5 s; (c) 1-LPI-based KT with CPI = 4.5 s.

References

[1] R. Zemmari, M. Daun, M. Feldmann and U. Nickel, "Maritime surveillance with GSM passive radar: Detection and tracking of small agile targets," *International Radar Symposium 2013*, Dresden, 2013.

[2] D.W O'Hagan., A. Capria, D.Petri, V.Kubica, M.Greco, F.Berizzi, A.G. Stove, "Passive Bistatic Radar (PBR) for harbour protection applications," *IEEE Radar Conference* 2012, Atlanta (GA), USA, May 2012.

[3] D. Langellotti, F. Colone, P. Lombardo, E. Tilli, M. Sedehi, and A. Farina, "Over the horizon maritime surveillance capability of DVB-T based passive radar," *European Radar Conference* 2014, Rome, Italy, Oct. 2014.

[4] T. Martelli, F. Colone, E. Tilli, A. Di Lallo, "Multi-Frequency Target Detection Techniques for DVB-T Based Passive Radar Sensors," *Sensors* 2016.

[5] H. Ma et al., "Maritime Moving Target Indication Using Passive GNSS-based Bistatic Radar," in *IEEE Transactions on Aerospace and Electronic Systems*, vol. 54, no. 1, pp. 115-130, Feb. 2018.

[6] M. Gashinova, L. Daniel, S. Hristov, X. Lyu, A. G. Stove, M. Cherniakov, "Design and Validation of a Passive Radar Concept for Ship Detection using Communication Satellite Signals," in *IEEE Trans. on Aerospace and Electronic Systems*, vol. 53, no. 6, pp. 3115-3134, Dec. 2017.

[7] K. S. Kulpa, and J. Misiurewicz, "Stretch Processing for Long Integration Time Passive Covert Radar," *CIE International Conference on Radar 2006*, Shanghai, 2006, pp. 1-4.

[8] J. M. Christiansen, K. E. Olsen and G. Weiß, "Coherent range and Doppler-walk compensation in PBR applications," *International Radar Symposium (IRS) 2014*, Gdansk, 2014, pp. 1-4.

[9] M. Radmard, H. Habibi, M. H. Bastani, and F. Behnia, "Target's range migration compensation in passive radar," *European Radar Conference 2009*, Rome, 2009, pp. 457-460.

[10] K. M. Scott, W. C. Barott, and B. Himed, "The keystone transform: Practical limits and extension to second order corrections," *IEEE Radar Conference 2015*, Arlington, VA, 2015.

[11] T. Shan, S. Liu, Y. D. Zhang, M. G. Amin, R. Tao, Y. Feng, "Efficient architecture and hardware implementation of coherent integration processor for digital video broadcast-based passive bistatic radar," *IET Radar, Sonar & Navigation*, vol. 10, no. 1, pp. 97-106, 1 2016.

[12] F. Pignol, F. Colone and T. Martelli, "Lagrange polynomial interpolation based Keystone Transform for passive radar," in *IEEE Transactions on Aerospace and Electronic Systems*, vol. PP, no. 99, pp. 1-1.

[13] P. Lombardo, and F. Colone, "Advanced processing methods for passive bistatic radar systems," in *Principles of Modern Radar: Advanced Radar Techniques*, W. L. Melvin, and J. A. Scheer, Raleigh, NC: SciTech Publishing, 2012.

[14] F. Colone, C. Palmarini, T. Martelli, E. Tilli, "Sliding extensive cancellation algorithm for disturbance removal in passive radar," in *IEEE Transactions on Aerospace and Electronic Systems*, vol. 52, no. 3, pp. 1309-1326, June 2016.

[15] F. Colone, D. Langellotti, and P. Lombardo, "DVB-T signal ambiguity function control for passive radars," *in IEEE Transactions on Aerospace and Electronic Systems*, vol. 50, no. 1, pp. 329-347, January 2014.